Hindawi
Journal of Nanomaterials
Volume 2020, Article ID 7379867, 11 pages
https://doi.org/10.1155/2020/7379867

Research Article

Electrical Trimming Characteristics of Polysilicon Nanofilms with Different Doping Concentrations and Deposition Temperatures

Xuebin Lu,[1] **Rui Weng**,[1] **Xiaowei Han**,[2,3] **Bin Yu**,[1] **and Bing Yang**[1]

[1]*Software and Microelectronics School, Harbin University of Science and Technology, Harbin 150080, China*
[2]*School of Computer and Information Engineering, Harbin Commerce University, Harbin 150080, China*
[3]*Heilongjiang Provincial Key Laboratory of Electronic Commerce and Information Processing, Harbin 150080, China*

Correspondence should be addressed to Xuebin Lu; lxbsw@126.com

Received 19 December 2018; Revised 5 December 2019; Accepted 30 December 2019; Published 24 February 2020

Academic Editor: Oscar Perales-Pérez

Polysilicon nanofilm (PSNF) can provide a large gauge factor and good temperature stability, which promotes their application in piezoresistive sensing devices. Electrical trimming is necessary to further improve the stability and matching of piezoresistive resistors after sensor fabrication. The advantages of PSNF are realized by first preparing PSNF samples with different doping concentrations and deposition temperatures. By applying an incremental DC current that is higher than the threshold current of the PSNF resistors, the PSNF resistors are trimmed and the resistance changes are measured. The results of electrical trimming show that the threshold current, trimming rate, and trimming error are related to the doping concentration and deposition temperature. According to tunneling piezoresistive theory and the interstitial-vacancy pair model, the experimental results are expounded. These results are useful for the design and fabrication of PSNF piezoresistive sensors.

1. Introduction

Polysilicon is an important material in CMOS transistors and MEMS sensors. The piezoresistive properties of polysilicon have been studied since the 1970s [1–3] and have been used in the design of piezoresistive pressure sensors.

In recent years, polysilicon nanofilm (PSNF, thickness of less than 100 nm) has received increasing attention. According to our previous research, PSNF has favorable performance because it has a remarkable tunneling piezoresistive effect [4, 5]. PSNF can play an important role as a pressure-sensitive material in MEMS sensors, especially in high-temperature piezoresistive sensors.

In this study, PSNF samples were prepared to investigate the effects of doping concentration and deposition temperature on the electrical trimming characteristics of the samples. The electrical trimming was performed by applying an incremental DC current to the PSNF resistors. The experimental results are explained by tunneling piezoresistive theory and the interstitial-vacancy (IV) pair model [6, 7].

2. Materials and Methods

2.1. Preparation of PSNF Sample with Different Doping Concentrations. Single crystal silicon of <111> orientation (thickness: 510 μm) was selected as the substrate, and then, an oxide layer (thickness: 860 nm) was cultured by thermal oxidation. The 80 nm thick PSNF samples were deposited on the silicon oxide layer at 620°C by low-pressure chemical vapor deposition (LPCVD). The samples were doped by ion implantation of boron with an energy of 20 keV and doses of 1.2×10^{15} cm^{-2}, 2.3×10^{15} cm^{-2}, 4.7×10^{15} cm^{-2}, and 8.2×10^{15} cm^{-2}, respectively. According to the solid solubility of boron ions in silicon, the doping concentrations of the samples were estimated to be 1.0×10^{20} cm^{-3}, 2.0×10^{20} cm^{-3}, 4.1×10^{20} cm^{-3}, and 7.1×10^{20} cm^{-3}, respectively. To electri-

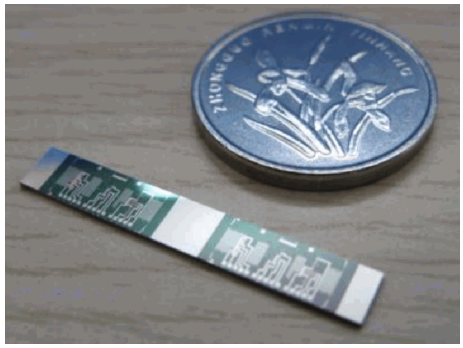

Figure 1: Photograph of the cantilever beam with PSNF piezoresistors.

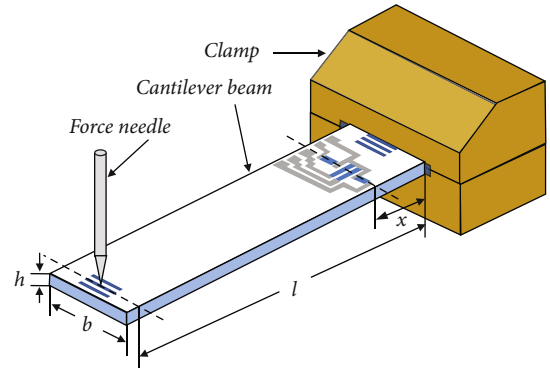

Figure 2: Schematic diagram of gauge factor test setup.

cally activate the boron ions, the samples were annealed under nitrogen protection for half an hour at 1080°C. The resistor patterns with a length ratio of 400 μm/100 μm were made by photolithography and wet etching. The aluminum film was then evaporated onto the silicon wafer to form electrodes. Finally, the cantilevers with PSNF resistors were obtained by photolithography. The final structure of the cantilever is 26 mm long and 4 mm wide, as shown in Figure 1.

2.2. Preparation of PSNF Sample with Different Deposition Temperatures. Monocrystalline silicon of <111> orientation (thickness: 510 μm) was used as a substrate to grow a SiO_2 layer (thickness: 860 nm) by thermal oxidation. PSNF samples with 80 nm thickness were deposited by LPCVD at temperatures of 580°C, 600°C, 620°C, and 670°C, respectively. Boron ions were injected into the PSNF with an energy of 20 keV and a dose of 2.3×10^{15} cm^{-2}. According to the solid solubility of boron ions in silicon, the doping concentrations of the samples were 2.0×10^{20} cm^{-3}. To electrically activate the boron ions, the samples were annealed at a temperature of 1080°C for 30 min under nitrogen protection. The PSNF was made into resistor patterns by lithography and wet etching. Next, the aluminum film was evaporated onto the silicon wafer to form electrodes and lead wires. Finally, the cantilever with PSNF resistors was obtained by photolithography. The cantilever beam is shown in Figure 1.

2.3. Measurement of PSNF Gauge Factor. The gauge factor test setup is shown in Figure 2. Either end of the cantilever beam is fixed by the clamp. The piezoresistors are connected to the electric instruments through Al electrodes. By applying the weight load to the front of the cantilever beam and measuring the variation of the piezoresistors, the gauge factor is obtained.

The strain $\varepsilon(x)$ can be calculated as follows:

$$\varepsilon(x) = \frac{6(l-x)}{bh^2 Y} P, \tag{1}$$

where x is the distance apart from the end of the cantilever clamp; l, b, and h are the cantilever length, width, and thickness, respectively (b, h<<l); Y is Young's modulus of monocrystalline silicon; and P is the weight load.

The initial resistance R_0 (without strain) and final resistance R (under strain) were measured using a Keithley 2000 digital multimeter. The gauge factor can be calculated as follows:

$$\mathrm{GF} = \frac{R - R_0}{R_0 \varepsilon(x)}. \tag{2}$$

2.4. Measurement of Electrical Trimming. The resistivity and sheet resistance of the PSNF resistors were measured using a four-probe resistivity tester. To perform electrical trimming, a trimming current was applied to the PSNF resistors for 30 s in each measurement. For PSNF samples having different doping concentrations, the amplitude of the trimming current was increased gradually; it was 5 mV for 1.0×10^{20} cm^{-3} and 2.0×10^{20} cm^{-3} doping samples and was 10 mV for 4.1×10^{20} cm^{-3} and 7.1×10^{20} cm^{-3} doping samples. For PSNF samples having different deposition temperatures, the amplitude of the trimming current was also increased incrementally and was 2 mV for the PSNF samples at 580°C and 620°C and was 5 mV for the PSNF samples at 600°C and 670°C, respectively. After each electrical trimming, the resistance values were measured using a Keithley 2000 digital multimeter.

3. Results and Discussion

3.1. Microstructure of PSNF with Different Doping Concentrations. The microstructure of PSNF with different doping concentrations was characterized using transmission electron microscopy (TEM), as shown in Figure 3(a). From the TEM image, it is seen that the grains are fine, with an average grain size of approximately 32 nm. To analyze the grain orientation, an X-ray diffraction (XRD) experiment was performed. The XRD of the PSNF samples is shown in Figure 3(b). In the XRD spectrum, the <111> peak is caused by the silicon substrate; there are no remarkable peaks attributed to other orientations. This indicates that the grains of PSNF are oriented randomly.

3.2. Microstructure of PSNF with Different Deposition Temperatures. The microstructure of PSNF with different deposition temperatures was characterized using scanning electron microscopy (SEM), as shown in Figures 4(a)–4(d).

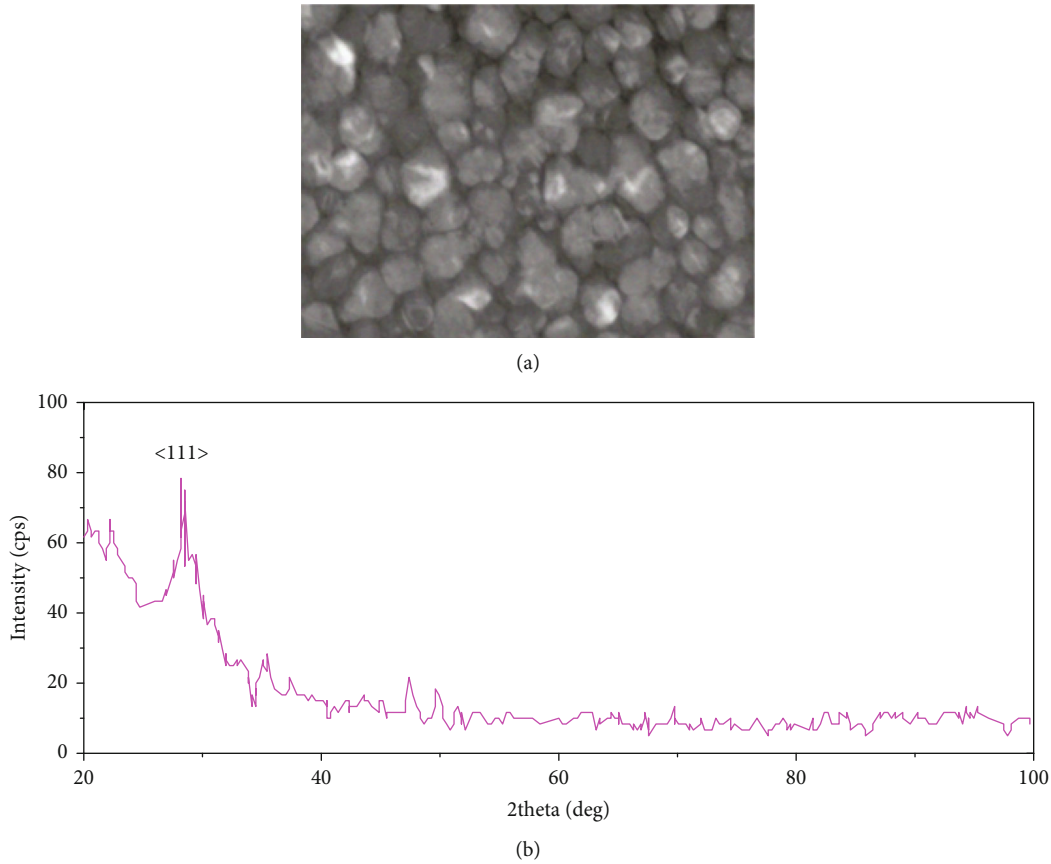

Figure 3: Microstructure characterization of PSNF with different doping concentrations: (a) TEM image; (b) XRD spectrum.

The SEM images show that the grain size increases with increasing deposition temperature. The XRD of the PSNF samples is shown in Figure 4(e). The XRD patterns indicate that there is less amorphous content in the 620°C films than in the other samples.

3.3. Gauge Factor of PSNF with Different Doping Concentrations. The relationship between the doping concentration and the gauge factor of PSNF is shown in Figure 5, where heavily doped PSNF has better piezoresistive characteristics (the gauge factor is from 33.31 to 38.40). The gauge factor is highest (38.40) for a doping concentration of 1.0×10^{20} cm^{-3}, and the gauge factor is weakly dependent on the doping concentration when the doping concentration is higher than 1.0×10^{20} cm^{-3}.

The polysilicon consists of monocrystalline silicon grains joined by grain boundaries, which can be seen in Figures 3 and 4. The grain boundary is a complex structure, usually consisting of a few atomic layers of disordered atoms. According to tunneling piezoresistive theory [4, 5], the resistance of PSNF (R_p) consists of the grain resistance (R_g) and the grain boundary resistance (R_b), as shown in Figure 6.

The gauge factor of R_p is the weighted average of the gauge factors of R_g and R_b. The grain boundary resistance has a remarkable piezoresistive effect compared to the grain resistance. Thus, the gauge factors of heavily doped PSNF are high. When the doping concentration is 1.0×10^{20} cm^{-3}, the highest gauge factor should come from the best weighted results. With an increasing doping concentration, the gauge factors of R_g and R_b are almost unchanged, and the PSNF gauge factor becomes stable.

3.4. Gauge Factor of PSNF with Different Deposition Temperatures. The relationship between deposition temperature and gauge factor of PSNF is shown in Figure 7, where the gauge factors are from 28.65 to 34.66. As the deposition temperature increases, the gauge factor of PSNF does not always decrease. The experimental data of PSNF samples at 620°C shows a special form, which is consistent with the results of Figure 4.

The polysilicon is composed of monocrystalline silicon grains joined by grain boundaries. The grain boundary is a type of complex structure, usually consisting of a few atomic layers of disordered atoms. High concentration defects and dangling bonds exist in grain boundaries. Therefore, grain boundaries play a key role in the nature of polysilicon material, and the grain boundary has a significant piezoresistive effect.

When the deposition temperature is lower than 620°C, the degree of crystallization of polysilicon is weak because of the low temperature. According to our tunneling piezoresistive theory [5], the grain boundary plays a dominant role in polysilicon, so the gauge factor is higher; when the

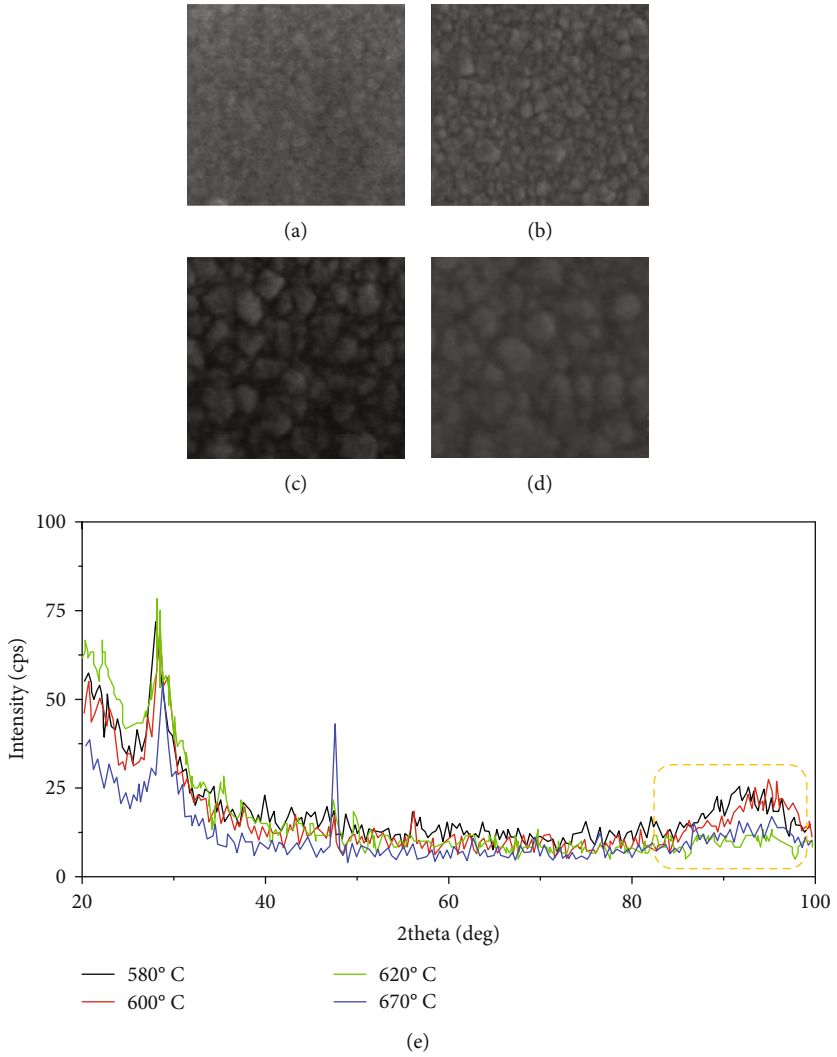

Figure 4: Microstructure characterization of PSNF with different deposition temperatures: (a) 580°C; (b) 600°C; (c) 620°C; (d) 670°C; (e) XRD spectrum.

deposition temperature is higher than 620°C, the degree of crystallization of polysilicon becomes stronger because of the high temperature. The impact of the grain boundary decreases, so that the gauge factor is lower. Therefore, 620°C is a special temperature point.

3.5. Electrical Trimming of PSNF with Different Doping Concentrations. The relationship of doping concentration with resistivity and sheet resistance of PSNF resistors is shown in Figure 8. With an increase of doping concentration, the resistivity and sheet resistance probably decrease exponentially. Under high doping concentrations ($\geq 4.1 \times 10^{20}\,\mathrm{cm}^{-3}$), the decrease of resistivity and sheet resistance becomes slower, which means that the ionization degree of boron ion decreases.

The electrical trimming characteristics of PSNF resistors under different doping concentrations is shown in Figure 9. When the trimming current is greater than the threshold current, the resistance value begins to fall. The decreasing slope of resistance is almost linear with the trimming current and is related to the doping concentration.

From Figure 9, the threshold current density of PSNF resistors is estimated and is shown in Figure 10, where the threshold current density has an approximately linear increase with an increase of the doping concentration.

The trimming rate (unit: ppm/A·cm^{-2}) is defined as the rate of change of normalized resistance under unit trimming current density. The trimming error is defined as the offset of actual resistance trimming deviated from the fitting straight line in the linear trimming region. According to Figure 9, the trimming rate and trimming error of PSNF piezoresistors with different doping concentrations are calculated and are shown in Figure 11, where the trimming rate and trimming error of PSNF resistors have an approximately exponential decrease with an increase of the doping concentration. This indicates that elevating the doping concentration can improve the trimming accuracy of PSNF resistors at the cost of a decreasing trimming rate.

As shown in Figures 3 and 4, polycrystalline silicon consists of monocrystalline silicon grains with grain boundaries connected. The grain boundary is a complex structure that

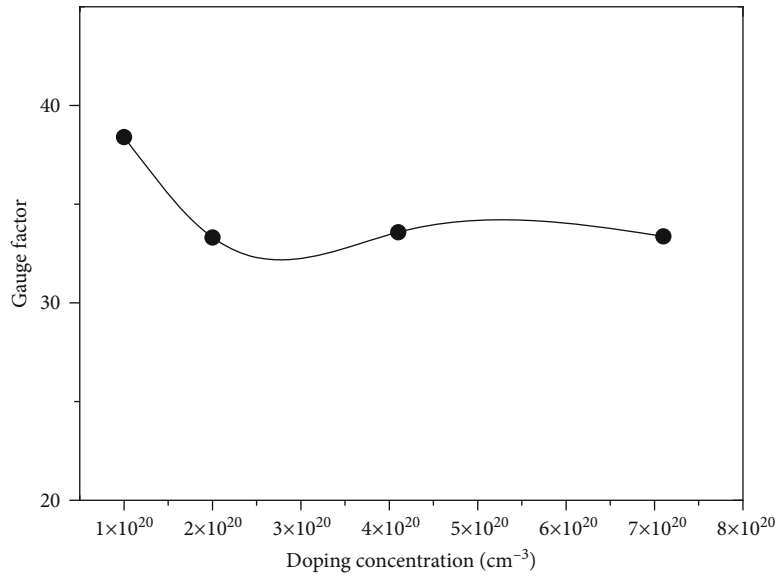

Figure 5: Gauge factor vs. doping concentration.

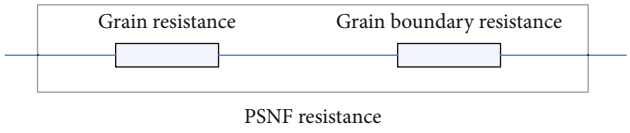

Figure 6: Resistance model of PSNF.

usually consists of disordered atomic layers. There are high concentration defects and suspensions in the grain boundary. Therefore, the grain boundary plays a key role in the properties of polysilicon materials.

The grain is seen as a small single crystal, and the properties of the grain boundary can be considered to be amorphous. The disordered state in amorphous silicon can be characterized as the accumulation of interstitial silicon atoms and vacancies, such as the IV pair model [6, 8], as shown in Figure 12. The grain boundary of PSNF can be modeled by the accumulation of IV pairs. The state of each IV pair depends on the number of adjacent IV pairs.

The grain boundary of PSNF is considered to be continuous amorphous layers. The number of IV pair interfaces is less than the number of the inner layers at the grain boundary. Compared with the grain resistance, the grain boundary resistance is higher. Under external energy excitation, there is high energy at the grain boundary. The IV pairs at grain boundary interfaces first recombine and then start a layer-by-layer recrystallization process from the interface toward the inner zone at the grain boundary. During recrystallization, the number of IV pairs decreases.

The IV model can be used to explain the characteristics of electrical trimming. As mentioned above, IV pairs at a grain boundary can recombine under external energy excitation. When using a small current that is less than the threshold current density, the generation and recombination of IV pairs coexist, resulting in dynamic equilibrium. When the applied current is greater than the threshold current, the large energy generated at the high-resistivity grain boundary leads to more recombination of the IV pairs, which reduces the number of defects. This reduces the number of scattering centers and increases the mobility of carriers on the grain boundary, resulting in a decrease of the resistance value.

From Figure 10, the threshold current density increases with an increase of the doping concentration. According to our tunneling piezoresistive theory, which is shown in Figure 6, the resistance of PSNF (R_p) consists of grain resistance (R_g) and grain boundary resistance (R_b). The resistivity of PSNF decreases with an increase of the doping concentration, which is mainly due to the decrease of R_b. According to Ohm's law, with an increasing doping concentration, a higher current is required in PSNF to generate enough energy for recombination of IV pairs at the grain boundary, because R_b decreases.

From Figure 11, the trimming rate and trimming error of PSNF decrease with an increase of the doping concentration. In addition, with an increase of the doping concentration, the number of IV pairs at grain boundaries decreases, which can be concluded because the resistivity of PSNF decreases with an increase of the doping concentration. According to the IV pair model, the state of each IV pair is dependent on the number of adjacent IV pairs. Obviously, reducing the number of IV pairs reduces the trimming rate and trimming error.

3.6. Electrical Trimming of PSNF with Different Deposition Temperatures. Figure 13 shows the electrical trimming characteristics of PSNF resistors under different deposition temperatures. In the electrical trimming experiments, the resistance value is reduced by adding a current that is greater than a certain threshold current on each tested PSNF resistor. The resistance values of trimmed PSNF resistors decrease almost linearly with an increase of the

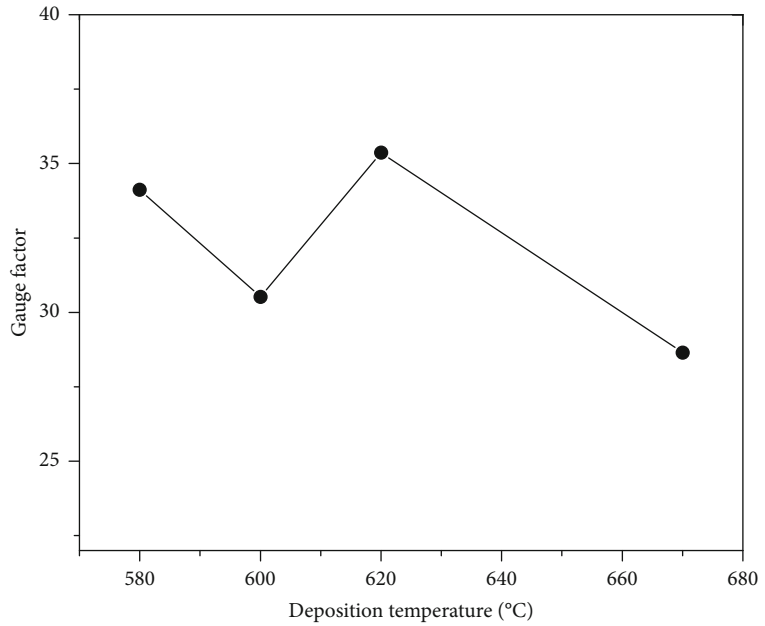

Figure 7: Gauge factor vs. deposition temperature.

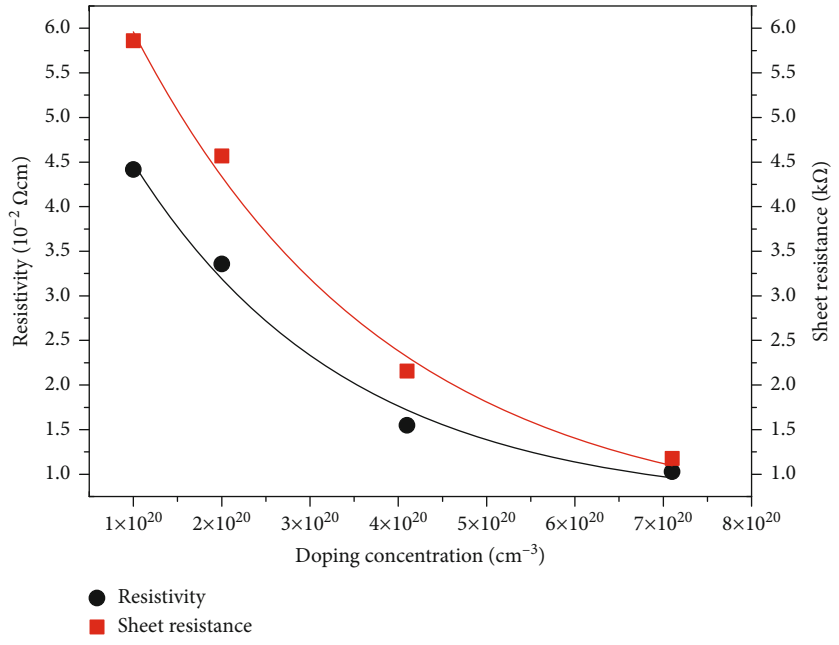

Figure 8: Resistivity and sheet resistance vs. doping concentration.

trimming current. The decreasing slope of resistance is related to the deposition temperature.

In PSNF, the grain is regarded as small single crystals, and the nature of the grain boundary can be considered to be amorphous. According to the work by Changzhi et al. [6], the disordered states in amorphous silicon can be characterized as the accumulation of interstitial silicon atoms and vacancies; grain boundaries of PSNF can be modeled by the accumulation of IV pairs, where the state of each IV pair is dependent on the number of neighboring IV pairs.

For polysilicon material, the grain boundary is considered to be comprised of continuous amorphous layers, and the number of IV pairs at grain boundary interfaces is lower than the number at the inner zones of grain boundaries. Under external energy excitation, where there is high current, the IV pairs at a grain boundary interface first recombine and then start a layer-by-layer recrystallization process toward the inner zone of the grain boundary. Through recrystallization, the number of IV pairs decreases [7, 9].

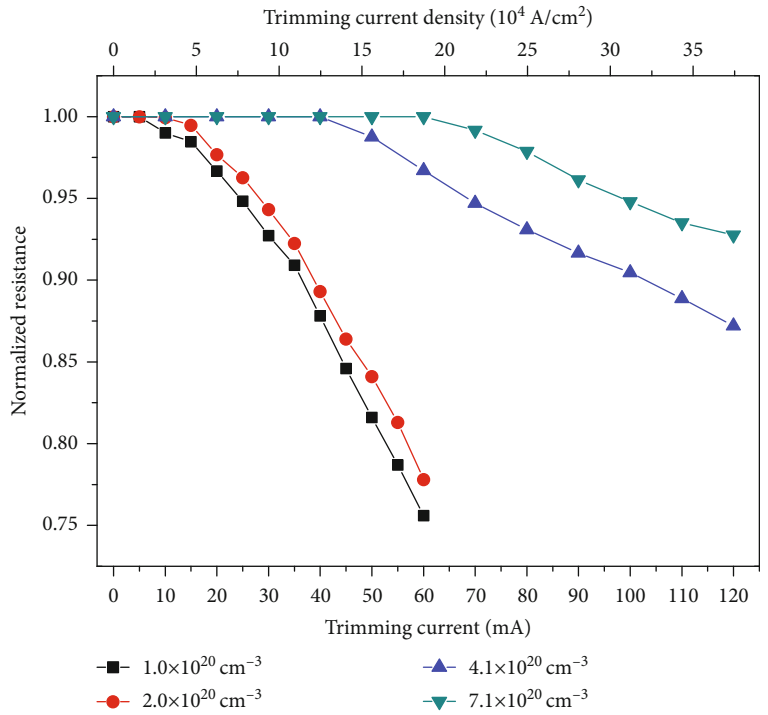

Figure 9: Normalized resistance vs. trimming current under different doping concentrations.

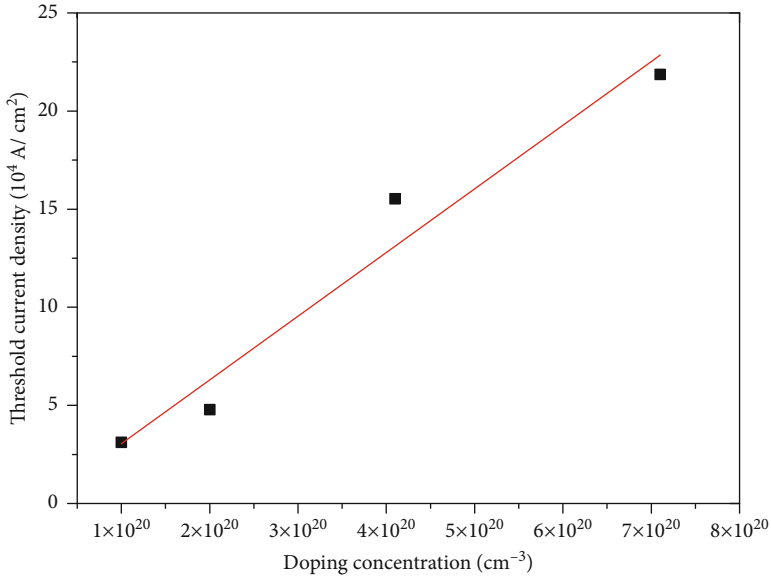

Figure 10: Threshold current density vs. doping concentration.

The characteristics of electrical trimming can be explained by the IV pair model. As mentioned above, the IV pairs at grain boundaries can recombine under external energy excitation. When a current that is lower than the threshold current density is applied, the generation and recombination of IV pairs coexist, causing a dynamic balance. When the applied current is higher than the threshold current density, the generated high energy at the high-resistivity grain boundary results in more recombination of IV pairs. The recombination of IV pairs can reduce the number of defects. Thus, this decreases the number of scattering centers and increases the carrier mobility at grain boundaries, thereby causing a decrease of the resistance values.

The threshold current densities of tested PSNF resistors are estimated from Figure 13 and are shown in Figure 14, where the threshold current density does not always increase with an increase of the deposition temperature. Datapoints at

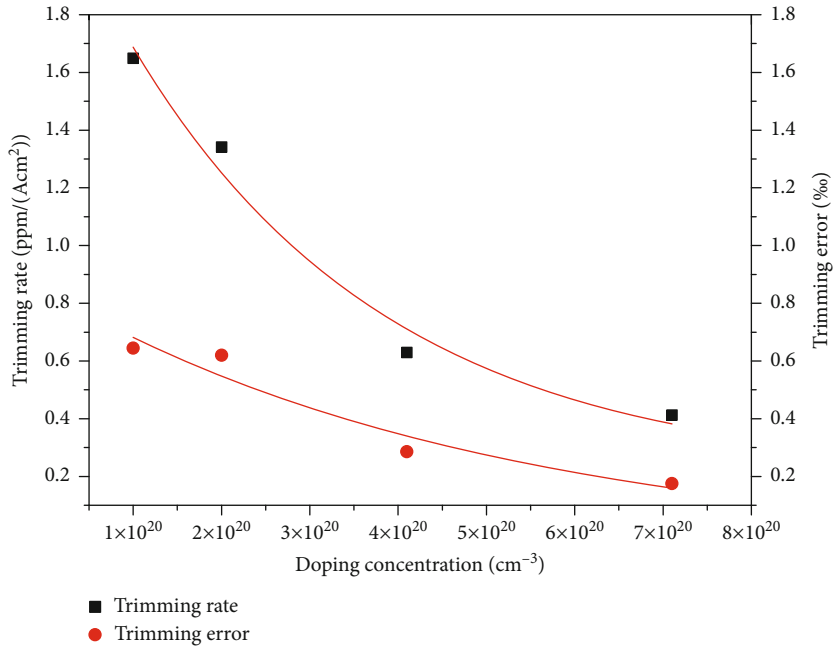

Figure 11: Trimming rate and trimming error vs. doping concentration.

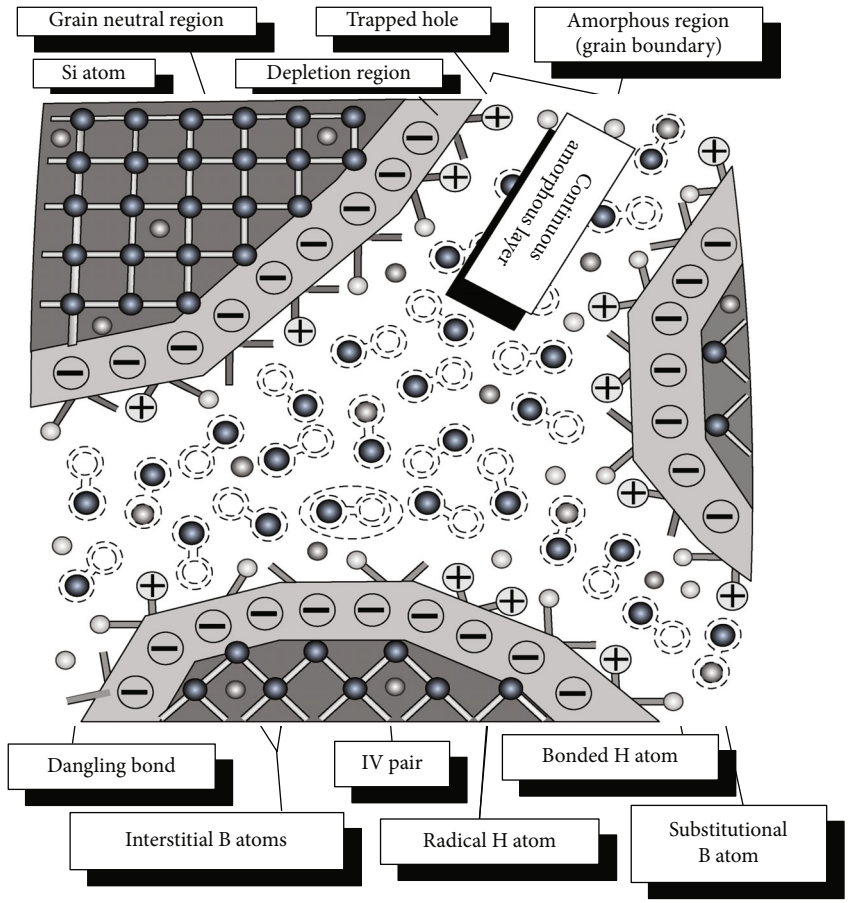

Figure 12: Interstitial-vacancy pair model.

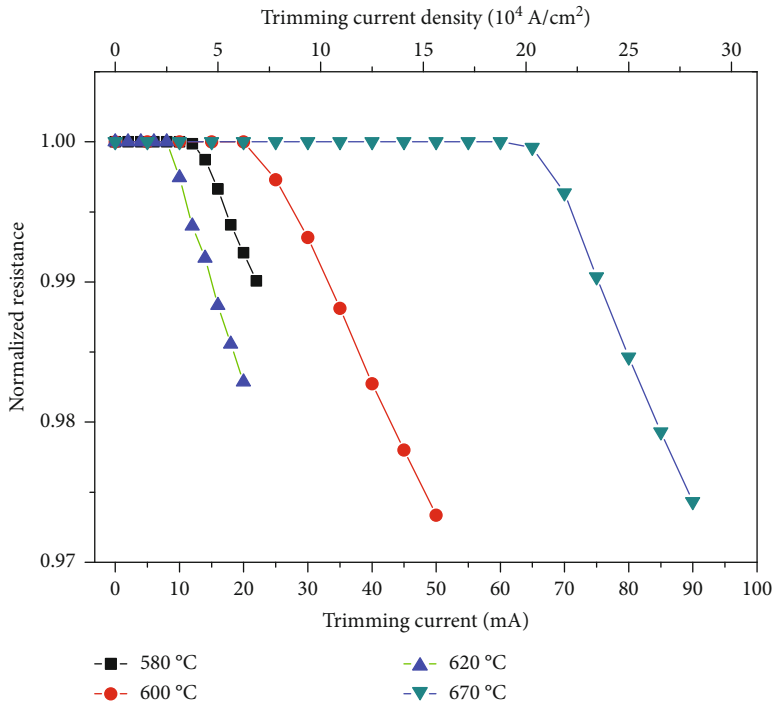

Figure 13: Normalized resistance vs. trimming current under different deposition temperatures.

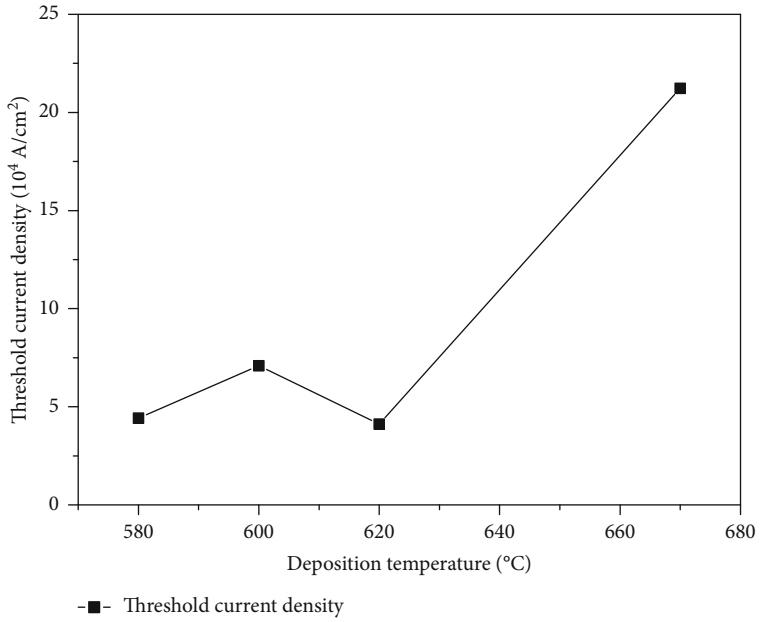

Figure 14: Threshold current density vs. deposition temperature.

620°C samples still show a special form, which could be from the special quality of PSNF samples deposited at 620°C.

In Figure 14, except for datapoints at 620°C, the threshold current density increases with an increase of the deposition temperature. An elevation of the deposition temperature can increase the degree of crystallinity, resulting in an increase of the grain size and a weakening of the grain boundary. The PSNF then requires a higher current to generate enough energy for recombination of IV pairs at the grain boundary. PSNF samples at a deposition temperature of 620°C have better piezoresistive properties, and the role of the grain boundary is significant. This means that there are more IV pairs at grain boundaries, and the smaller current density may lead to recombination of IV pairs and a decrease of the threshold current density of PSNF samples at 620°C.

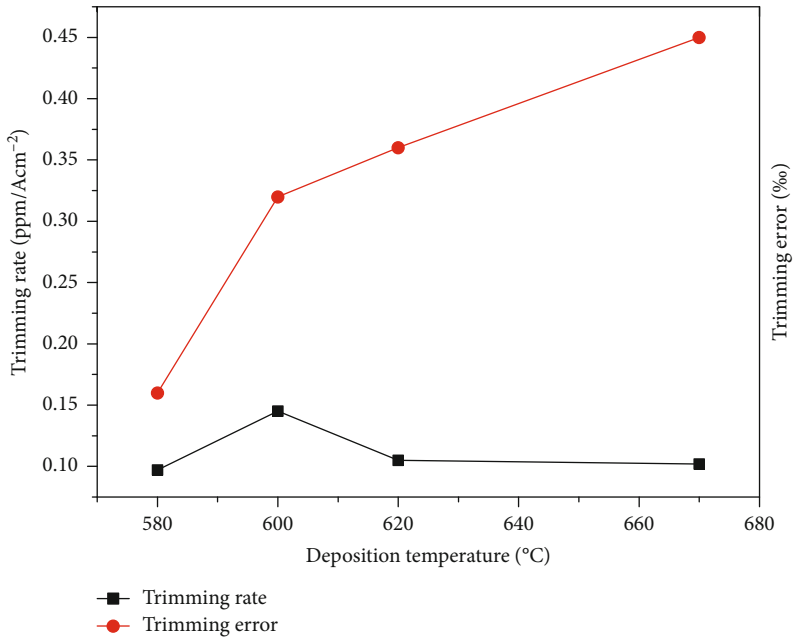

Figure 15: Trimming rate and trimming error vs. deposition temperature.

The trimming rate and trimming error of the PSNF resistors with different deposition temperatures (see Figure 13) are calculated, as shown in Figure 15.

In Figure 15, the trimming rate is from 0.102 ppm/A·cm^{-2} to 0.145 ppm/A·cm^{-2}, and the trimming error is from 0.16‰ to 0.45‰. From Figure 13, the trimming rate is weakly dependent on the deposition temperature, and the trimming error increases with an increase of the deposition temperature. It can be seen from Figures 14 and 15 that an increase of the trimming current causes an increase of the trimming error.

4. Conclusions

In this study, the electrical trimming characteristics of PSNF were investigated. The experimental results show that PSNF can provide favorable piezoresistive characteristics. By applying a current that is higher than a certain threshold current on each tested PSNF resistor, the resistance value decreased in an almost linear manner. The threshold current, trimming rate, and trimming error are related to the doping concentration and deposition temperature. The experimental results are explained by tunneling piezoresistive theory and the IV pair model. The conclusions indicate that electrical trimming is an especially useful method for correcting PSNF resistance.

Data Availability

The origin data used to support the findings of this study are available from the corresponding author upon request.

Conflicts of Interest

The authors declare that there is no conflict of interest regarding the publication of this paper.

Acknowledgments

We would like to thank Editage (http://www.editage.com) for English language editing. This work was supported by the Natural Science Foundation of Heilongjiang Province (grant numbers F2018018 and F2018020).

References

[1] Y. Onuma and K. Sekiya, "Piezoresistive properties of polycrystalline thin films," *Japanese Journal of Applied Physics*, vol. 11, pp. 420-421, 1974.

[2] E. Luder, "Polycrystalline silicon-based sensors," *Sensors and Actuators*, vol. 11, no. 1, pp. 9–23, 1986.

[3] D. Schubert, W. Jenschke, T. Uhlig, and F. M. Schmidt, "Piezoresistive properties of polycrystalline and crystalline silicon films," *Sensors and Actuators*, vol. 11, no. 2, pp. 145–155, 1987.

[4] R. Chuai, X. Liu, and M. Huo, "Influence of doping level on the gauge factor of polysilicon nano-film," *Journal of Semiconductors*, vol. 27, no. 7, pp. 1230–1235, 2006.

[5] X. B. Lu, X. W. Liu, R. Y. Chuai, C. Z. Shi, M. X. Huo, and W. P. Chen, "Analysis of tunneling piezoresistive effect of p-type polysilicon Nanofilms," *Advanced Materials Research*, vol. 60-61, pp. 89–93, 2009.

[6] C. Shi, X. Liu, and R. Chuai, "DC electrical trimming characteristics of polysilicon nanofilms with different doping concentrations," in *Proceeding of the 4th IEEE international Conference on Nano/Micro Engineered and Molecular Systems*, pp. 686–689, Shenzhen, China, Jan. 2009.

[7] Y. Amemiya, T. Ono, and K. Kato, "Electrical trimming of heavily doped polycrystalline silicon resistors," *IEEE Transactions on Electron Devices*, vol. 26, no. 11, pp. 1738–1742, 1979.

[8] L. A. Marqués, L. Pelaz, J. Hernández, J. Barbolla, and G. H. Gilmer, "Stability of defects in crystalline silicon and their role in amorphization," *Physical Review B*, vol. 64, no. 4, pp. 1–9, 2001.

[9] N. Yu, G. Yong, and C. Zhiming, "Resistivity instability in polysilicon resistors under metal interconnects and its suppression by compensating ion implantation," *Chinese Journal of Semiconductors*, vol. 22, no. 4, pp. 511–515, 2001.